Effect of probe geometry on transsceral diffuse optical spectroscopy

Svenmarker, Pontus; Xu, Can; Andersson-Engels, Stefan; Krohn, Jørgen

Published in:
Biomedical Optics Express

2011

Effects of probe geometry on transscleral diffuse optical spectroscopy

Pontus Svenmarker,[1] Can T. Xu,[1] Stefan Andersson-Engels,[1] and Jørgen Krohn[2,3]

[1]*Department of Physics, Lund University, P.O Box 118, SE-221 00 Lund, Sweden*
[2]*Department of Clinical Medicine, Section of Ophthalmology, University of Bergen, N-5020 Bergen, Norway*
[3]*Department of Ophthalmology, Haukeland University Hospital, N-5021 Bergen, Norway*
pontus.svenmarker@fysik.lth.se

Abstract: The purpose of this study was to investigate how the geometry of a fiber optic probe affects the transmission and reflection of light through the scleral eye wall. Two geometrical parameters of the fiber probe were investigated: the source-detector distance and the fiber protrusion, i.e. the length of the fiber extending from the flat surface of the fiber probe. For optimization of the fiber optic probe geometry, fluorescence stained choroidal tumor phantoms in *ex vivo* porcine eyes were measured with both diffuse reflectance- and laser-induced fluorescence spectroscopy. The strength of the fluorescence signal compared to the excitation signal was used as a measure for optimization. Intraocular pressure (IOP) and temperature were monitored to assess the impact of the probe on the eye. For visualizing any possible damage caused by the probe, the scleral surface was imaged with scanning electron microscopy after completion of the spectroscopic measurements. A source-detector distance of 5 mm with zero fiber protrusion was considered optimal in terms of spectroscopic contrast, however, a slight fiber protrusion of 0.5 mm is argued to be advantageous for clinical measurements. The study further indicates that transscleral spectroscopy can be safely performed in human eyes under *in vivo* conditions, without leading to an unacceptable IOP elevation, a significant rise in tissue temperature, or any visible damage to the scleral surface.

OCIS codes: (300.6550) Spectroscopy, visible; (170.6510) Spectroscopy, tissue diagnostics; (170.3890) Medical optics instrumentation; (170.6280) Spectroscopy, fluorescence and luminescence; (290.1990) Scattering, diffusion

References and links

1. J. Q. Brown, K. Vishwanath, G. M. Palmer, and N. Ramanujam, "Advances in quantitative UV-visible spectroscopy for clinical and pre-clinical application in cancer," Curr. Opinion Biotechnol. **20**, 119–131 (2009).
2. I. Rennie, "Things that go bump in the light. the differential diagnosis of posterior uveal melanomas," Eye **16**, 325–346 (2002).
3. J. A. Shields, A. Mashayekhi, R. A. Seong, and C. l. Shields, "Pseudomelanomas of the posterior uveal tract: The 2006 Taylor R. Smith Lecture," Retina **25**, 767–771 (2005).
4. J. Krohn, C. T. Xu, P. Svenmarker, D. Khoptyar, and S. Andersson-Engels, "Transscleral visible/near-infrared spectroscopy for quantitative assessment of melanin in a uveal melanoma phantom of ex vivo porcine eyes," Exp. Eye Res. **90**, 330–336 (2010).

#151319 - $15.00 USD Received 18 Jul 2011; revised 18 Sep 2011; accepted 18 Sep 2011; published 7 Oct 2011

5. C. T. Xu, P. Svenmarker, S. Andersson-Engels, and J. Krohn, "Transscleral visible/near-infrared spectroscopy for quantitative assessment of haemoglobin in experimental choroidal tumours," Acta Ophthalmol., http://onlinelibrary.wiley.com/doi/10.1111/j.1755-3768.2010.02037.x/full.
6. S. L. Jacques and B. W. Pogue, "Tutorial on diffuse light transport," J. Biomed. Opt. **13**, 041302 (2008).
7. T. Durduran, R. Choe, W. B. Baker, and A. G. Yodh, "Diffuse optics for tissue monitoring and tomography," Rep. Prog. Phys. **73**, 076701 (2010).
8. M. S. Patterson, S. Andersson-Engels, B. C. Wilson, and E. K. Osei "Absorption-spectroscopy in tissue-simulating materials - a theoretical and experimental-study of photon paths," Appl. Opt. **34**, 22–30 (1995).
9. T. J. Pfefer, L. S. Matchette, A. M. Ross, and M.N. Ediger "Selective detection of fluorophore layers in turbid media: the role of fiber-optic probe design," Opt. Lett. **28**,120-122 (2003).
10. C. F. Zhu, Q. Liu, and N. Ramanujam "Effect of fiber optic probe geometry on depth-resolved fluorescence measurements from epithelial tissues: a Monte Carlo simulation" J. Biomed. Opt. **8**, 237-247 (2003).
11. M. Hammer, A. Roggan, D. Schweitzer, and G. Mller, "Optical properties of ocular fundus tissues - an in vitro study using the double-integrating-sphere technique and inverse monte carlo simulation," Phys. Med. Biol. **40**, 963–978 (1995).
12. M. Maus, *Principles and Practice of Ophthalmology: Clinical Practice* (W.B. Saunders, 1994), vol. 3.
13. I. Schoemaker, P. P. W. Hoefnagel, T. J. Mastenbroek, C. F. Kolff, S. Schutte, F. C. T. van der Helm, S. J. Picken, A. F. C. Gerritsen, P. A. Wielopolski, H. Spekreijse, and H. J. Simonsz, "Elasticity, viscosity, and deformation of orbital fat," Investigative Ophthalmol. Visual Sci. **47**, 4819–4826 (2006).
14. H. Hh and M. Schwanengel, "Continuous measurement of intraocular pressure by the codman micro sensor for several days - a case report," Klin. Monatsbl. Augenheilkd. **215**, 186–196 (1999).
15. G. Zijlstra, Willem, A. Buursma, and O. W. van Assendelft, *Visible and Near Infrared Absorption Spectra of Human and Animal Haemoglobin - determination and application* (VSP, 2000).
16. K. Palmer and D. Williams, "Optical-properties of water in near-infrared," J. Opt. Soc. Am. **64**, 1107–1110 (1974).
17. N. Kollias and A. Baqer, "Spectroscopic characteristics of human melanin invivo," J. Investigative Dermatol. **85**, 38–42 (1985).
18. R. Marchesini, A. Bono, and M. Carrara, "In vivo characterization of melanin in melanocytic lesions: spectroscopic study on 1671 pigmented skin lesions," J. Biomed. Opt. **14** (2009).
19. B. Cameron, N. Saffra, and M. Strominger, "Laser in situ keratomileusis-induced optic neuropathy," Ophthalmology **108**, 660–665 (2001).
20. Y. Ti and W.-C. Lin, "Effects of probe contact pressure on in vivo optical spectroscopy," Opt. Express **16**, 4250–4262 (2008).
21. K. C. Y. Chan, A. Poostchi, T. Wong, E. A. Insult, N. Sachdev, and A. P. Wells, "Visual field changes after transient elevation of intraocular pressure in eyes with and without glaucoma," Ophthalmology **115**, 667–672 (2008).
22. J. H. Prince, *Anatomy and histology of the eye and orbit in domestic animals* (C. C. Thomas, Springfield, Ill., 1960).
23. T. Olsen, S. Aaberg, D. Geroski, and H. Edelhauser, "Human sclera: thickness and surface area," Am. J. Ophthalmol. **125**, 237–241 (1998).
24. R. E. Norman, J. G. Flanagan, S. M. K. Rausch, I. A. Sigal, I. Tertinegg, A. Eilaghi, S. Portnoy, J. G. Sled, and C. R. Ethier, "Dimensions of the human sclera: thickness measurement and regional changes with axial length," Exp. Eye Res. **90**, 277–284 (2010).
25. T. Olsen, S. Sanderson, X. Feng, and W. Hubbard, "Porcine sclera: thickness and surface area," Investigative Ophthalmol. Visual Sci. **43**, 2529–2532 (2002).
26. J. Krohn and T. Bertelsen, "Light microscopy of uveoscleral drainage routes after gelatine injections into the suprachoroidal space," Acta Ophthalmol. Scan. **76**, 521–527 (1998).
27. B. W. Pogue and M. S. Patterson, "Review of tissue simulating phantoms for optical spectroscopy, imaging and dosimetry," J. Biomed. Opt. **11** (2006).
28. J. Swartling, J. Dam, and S. Andersson-Engels, "Comparison of spatially and temporally resolved diffuse-reflectance measurement systems for determination of biomedical optical properties," Appl. Opt. **42**, 4612–4620 (2003).
29. J. Krohn, O. R. Monge, T. N. Skorpen, S. J. Mørk, and O. Dahl, "Posterior uveal melanoma treated with I-125 brachytherapy or primary enucleation," Eye **22** 1398-1403 (2008).

1. Introduction

Optical spectroscopy has been used as a supplementary technique for detection and characterization of cancer in many human organs [1]. Choroidal melanoma is the most common primary malignant eye tumor, but a variety of other benign and malignant tumors may develop in the eye and pose diagnostic problems [2, 3]. Recently, we have shown that transscleral spectroscopy is

#151319 - $15.00 USD Received 18 Jul 2011; revised 18 Sep 2011; accepted 18 Sep 2011; published 7 Oct 2011

a feasible method for predicting the content of both melanin and hemoglobin in experimental choroidal tumors [4, 5]. The homogeneous structure of the sclera and the location of various choroidal tumors immediately underneath it, suggest that a transscleral approach is the most appropriate way to perform optical spectroscopy of intraocular tumors.

The wavelengths which can be used to probe optically thick tissues are limited by the scattering and absorption properties of the tissue. It is known that light of longer wavelengths, in general, has a lower attenuation than light of shorter wavelengths and thus a better penetration [6]. Many biologically important chromophores have specific absorption imprints residing within the shorter wavelength regions. Thus for spectroscopy measurements, a trade-off between penetration, signal-to-noise ratio and chromophore specificity and sensitivity needs to be considered. In addition to the wavelengths of the probe light, the source-detector distance is another important factor to consider for suitable depth penetration [7, 8]. Given the optical properties (reduced scattering coefficient, μ_s', and absorption coefficient, μ_a) of a tissue, the source-detector distance will directly influence the depth of the sampled volume, i.e. a large source-detector distance leads to a deeper sampled volume than a small source-detector distance [9, 10]. For measurements of the deeper situated regions within tissues, it is therefore important to select a suitable source-detector distance to maximize the spectroscopic contrast, i.e. the relative amount of photons which have interrogated the deeper situated tissue layers compared to the photons which have only propagated through the superficial layers.

The main purpose of this study was to develop a fiber optic probe suitable for being handheld during *in vivo* ocular spectroscopy and to optimize its parameters for transmitting and receiving light through the scleral eye wall. With the aim to measure blood, water and melanin concentrations, the spectral range needs to cover at least 600-1000 nm to include the imprints from the different chromophores. In our previous studies, the source-detector distance was first roughly estimated using Monte-Carlo simulations [4, 5]. Since few reports exist on optical properties of ocular tissues over a wide spectrum [11], the simulation results were only regarded as an estimate. To investigate this further, we here present experimental data with different source-detector distances. In addition, different fiber protrusions, i.e. the length of the fiber extending from the flat surface of the fiber probe are investigated. Protruding fibers will change the eye curvature and/or compress the scleral substance, which in turn may influence light transmission through the tissue. Benefits with slightly protruding fibers are that the probe can be more securely held in place and that temporary fine spots are created on the scleral surface, which can be used as a visual confirmation of the probe placement. For the different fiber probe configurations, the spectroscopic contrast was experimentally determined in *ex vivo* tissue phantom models with specific fluorescence labeling, using diffuse reflectance spectroscopy and laser-induced fluorescence. This provided a way to optimize the geometry of a handheld fiber optic probe for maximum spectroscopic contrast and signal-to-noise ratio, which also would be robust enough to clinically monitor intraocular tumors.

2. Materials and methods

2.1. Porcine eyes

Eyes from domestic pigs were obtained from a local abattoir. Pigs with a live weight of about 75 kg and an age of 6-7 months were used for the study. The eyes were removed within 12 hours postmortem and stored at 4 °C in a moist chamber until preparation. All experiments were performed within 4-5 days after the death of the animals.

2.2. Preparation of the tumor phantom

The methods for the preparation of tumor phantoms have previously been described in detail elsewhere [4, 5]. Briefly, each eye was prepared for injection under a dissecting microscope.

#151319 - $15.00 USD Received 18 Jul 2011; revised 18 Sep 2011; accepted 18 Sep 2011; published 7 Oct 2011

After removal of conjunctiva, muscles and other excess tissues, a 3-mm scleral incision was made 7.5 mm anterior to the optic nerve insertion. The injection was done with a 2-ml syringe connected to a cannula, with a blunt and flat tip, that was gently pushed through the sclerotomy and 3-4 mm anteriorly. A mixture of porcine skin gelatin powder (G1890; Type A; Sigma-Aldrich, St. Louis, MO) and titanium dioxide (TiO_2) (T8141; Sigma-Aldrich, St. Louis, MO) in distilled water was stirred with a magnetic bar for 15 minutes at 37°C until a homogeneous white suspension was obtained. By adding appropriate amounts of human venous blood (from one healthy volunteer) and the fluorophore Dy-781 (Dy-781; Dyomics GmbH, Jena, Germany) to the gelatin-TiO_2 suspension, samples with the final concentrations of 15% (wt/vol) gelatin, 10 mg/ml TiO_2, 5% (vol/vol) blood, and 0.5 µM Dy-781 were made. The suspensions were kept in a water bath at 37°C and stirred gently for another 2 minutes. Immediately prior to injection, the samples were placed in a warm vacuum chamber, and air bubbles trapped inside the suspension were eliminated by evacuating the chamber to a pressure of 0.25 bar for 1 minute. Then, 0.75 ml of the freshly prepared gelatin suspension was slowly injected into the suprachoroidal space between the sclera and the choroid. Immediately after the injection, the scleral incision was closed with a preplaced suture, and the eye was put into cold saline (5°C) to complete the gelation of the phantom. A cross section of an eye with a tumor phantom is shown in Fig. 1.

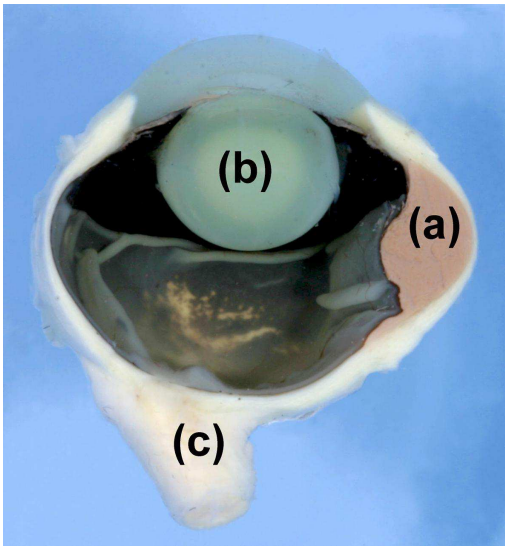

Fig. 1. Photograph of a cross-sectioned porcine eye. (a) Choroidal tumor phantom in the suprachoroidal space. Note that the phantom is in close contact with the surrounding tissues. (b) The crystalline lens in the anterior segment of the eye. (c) The optic nerve entering the posterior pole of the eye.

2.3. Spectroscopy and fluorescence equipment

The optical setup is schematically illustrated in Fig. 2. A high power projector quartz tungsten halogen lamp (Oriel Simplicity 66765; Newport Corporation, Irvine, CA) produced a smooth wide spectrum across the visible and near-infrared spectral region with little UV radiation. A low-noise power supply, specified to generate less than 0.05% current ripple, was used to drive the lamp, giving an intensity fluctuation of less than 2% over the usable spectrum during a measurement session of 30 minutes. Between two consecutive measurements, the fluctuations

#151319 - $15.00 USD Received 18 Jul 2011; revised 18 Sep 2011; accepted 18 Sep 2011; published 7 Oct 2011

were less than 0.1%. The total output power over the entire spectral range from the lamp was 300 mW, of which 15 mW was successfully coupled into a 600-µm fiber (BFL48-600; Thorlabs, Newton, NJ). The fiber was used to deliver the light to the sclera and a second similar fiber collected the light. Both fibers were integrated into a custom made probe designed for *in vivo* use (described in detail below). For this study, the probe was mounted on a micrometer-translator stage (CVI Melles Griot; Albuquerque, NM), which enabled it to be translated vertically. During all measurements, the pressure needed to applanate (flatten) the scleral surface by the end of the probe was monitored by placing the eye on an electronic scale (Kern 572; Kern & Sohn GmbH, Balingen, Germany). A barium sulfate ($BaSO_4$) disc (SRS-99-010; Oriel Corporation, Stratford, CT) was used as optical reflectance reference standard for the system. Detection was performed by a fiber-coupled spectrometer (QE65000; Ocean Optics, Dunedin, FL). It was configured with a 50 μm wide slit and a grating covering 350-1100 nm, giving a spectral resolution of at least 2.5 nm full width half maximum (FWHM).

Sequentially to the spectroscopy measurements, laser induced fluorescence could be measured. As excitation source, a 785-nm fiber-coupled diode laser (L785P100; Thorlabs, Newton, NJ), giving an output power of 25 mW, was used to irradiate the eye through the sclera. An 810-nm interference filter with a FWHM of 12 nm (S10-810-S; Newport Corporation, Irvine, CA), placed in the path between the collection fiber and the spectrometer, attenuated the excitation light to a level which allowed simultaneous detection of the fluorescence and the excitation light.

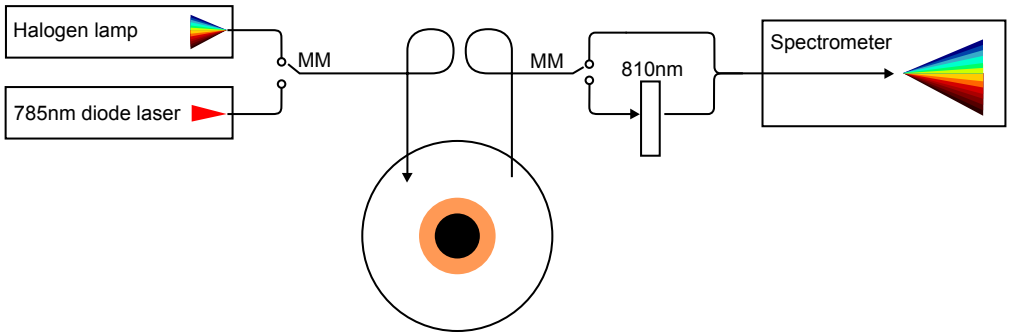

Fig. 2. Optical setup used during the experiments. A fiber-coupled halogen lamp delivered a wide spectrum covering the visible and near-infrared spectral regions through a multi-mode (MM) fiber (600 µm core) to the eye. Light was collected with a second multi-mode fiber and coupled to a spectrometer for spectroscopy measurements. Sequentially, a 785 nm diode laser was used together with an 810-nm interference filter, which attenuated the excitation light to a level were both the fluorescence and the excitation signal could be measured simultaneously.

2.4. Fiber probe configurations

Four different probes were constructed for the study. The probes were made of black, light-absorbing polyoxymethylene (Homopolymer acetal rods; Röchling Sustaplast KG, Lahnstein, Germany) and shaped like a cylinder with a length of 35 mm and a diameter of 10 mm. A schematic illustration of the probe can be seen in Fig. 3. Along the cylinder axis, two in-line holes (each with a diameter of 1.2 mm) made it possible to continuously adjust the fiber position. The hole diameter was set to fit the fiber diameter including the polymer coating. At the distal end of the fibers, approximately 5 mm of the polymer coating was removed, resulting in two fibers, each 600 μm in diameter, being in contact with the tissue during the measurements.

#151319 - $15.00 USD Received 18 Jul 2011; revised 18 Sep 2011; accepted 18 Sep 2011; published 7 Oct 2011

Each probe was made with a specific center-to-center source-detector distance of 3, 4, 5 and 6 mm, respectively. Two plastic screws (each with a diameter of 3 mm), placed 5 mm from the proximal end of the probe, were used to gently fix the fibers in the correct position. For the study, the protrusion of the optical fibers from the distal end of the probe were set to 0, 0.5, 1.0 or 1.5 mm. To facilitate the exact positioning of the fibers, standards made of thin metal plates with holes for the fibers and with corresponding thicknesses to the fiber protrusion were used.

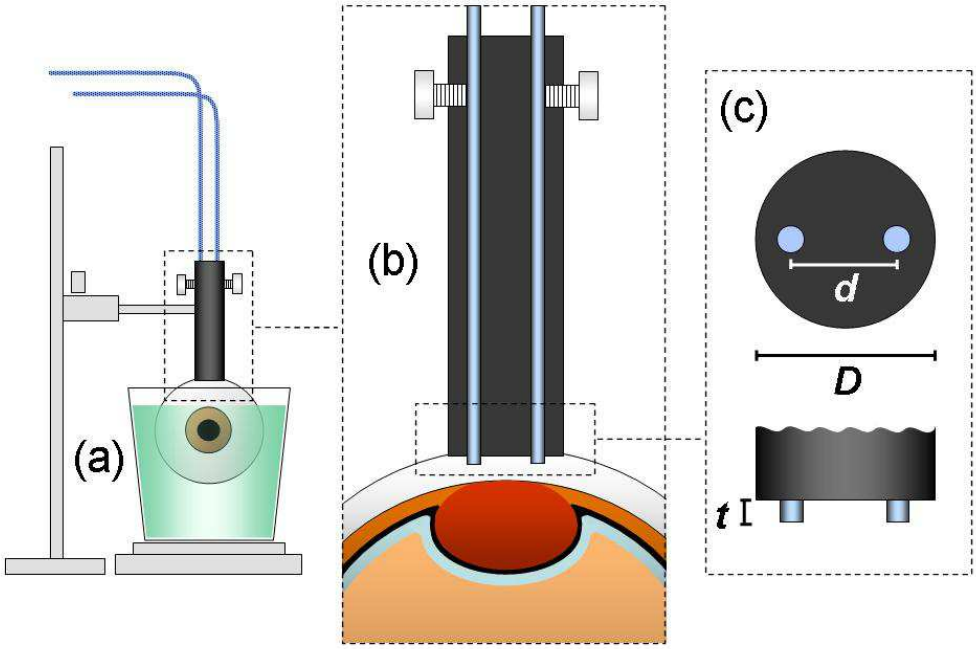

Fig. 3. Schematic illustration of the experimental setup and the principle of transscleral diffuse optical spectroscopy. (a) Porcine eye in a gelatin-filled plastic container placed on an electronic scale. (b) Cross section of the probe and the eye. The optical fibers (for incident and detected light) are fixed by two plastic screws and centered on the scleral surface over the tumor phantom. The phantom (red) is located in the suprachoroidal space between the sclera (white) and the retina and retinal pigment epithelium (light blue and black). (c) Front and side view of the probe end. The fiber protrusion t, from the distal end of the probe, can be varied between 0, 0.5, 1.0 and 1.5 mm. The source-detector distance d equals 3, 4, 5 or 6 mm for the four different probes used. The diameter D of the probe itself is 10 mm.

2.5. Measurement procedures

A total of six solitary intraocular tumor phantoms were made in six different eyes. B-scan ultrasonography (Echoscan US-3000; Nidek Co. Ltd., Gamagori, Japan) was performed to determine the size and shape of the phantoms. For accurate placement of the fiber probe, transillumination was used to outline the phantom borders by the shadow casted on the subadjacent sclera. Thereafter, the eye was placed in a transparent plastic container with 30 ml of congealed 10% (wt/vol) gelatin (Fig. 4). On the surface of the gelatin gel, a hemispherical cavity was made to hold the eye in place with adjacent physiological tension. The gelatin cup was designed to

#151319 - $15.00 USD Received 18 Jul 2011; revised 18 Sep 2011; accepted 18 Sep 2011; published 7 Oct 2011

match the volume of the human orbita [12] and the elasticity and viscosity of orbital tissues [13]. The fiber probe was carefully placed on the scleral surface, over the central portion of the phantom, and gradually depressed until the end of the probe applanated the scleral curvature (Fig. 3(b) and Fig. 4). Once the fiber probe was positioned, spectroscopy was performed followed by a fluorescence measurement. For the first three eyes, this procedure was repeated with four different fiber probes with source-detector distances of 3, 4, 5 and 6 mm, respectively, and with a fiber protrusion of 1.0 mm. For the last three eyes, the fibers protruded either 0, 0.5, 1.0 or 1.5 mm with a fixed source-detector distance of 5 mm. The integration time for the spectroscopy measurements ranged from 200 milliseconds to 10 seconds and was chosen as long as possible without saturating the detector. For the fluorescence measurements, a 10 seconds integration time was chosen. A reference standard spectrum was recorded between each measurement.

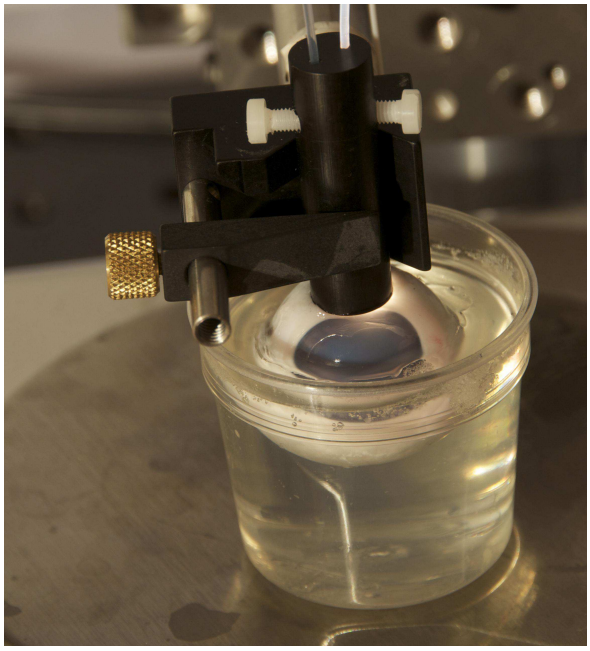

Fig. 4. Photograph of a porcine eye placed in the gelatin cup and applanated by the fiber probe mounted on the micrometer-translator stage.

2.6. Spectroscopic contrast through fluorescence measurements

To evaluate how much the light interrogated the tumor phantom, rather than merely the superficial scleral tissue for the different probe configurations, the fluorescence from the stained phantoms and the transmitted excitation light were measured. By comparing the two signals, it is possible to estimate the spectroscopic contrast in terms of how much the light interacted with the tumor phantom and the sclera, respectively. A maximum contrast would occur if all the light interacted with the phantom volume. As a measure of the spectroscopic contrast, the contrast function, Γ, was chosen to be the fluorescence signal divided by the excitation signal and given as

$$\Gamma = \frac{\int_{800}^{820} S\, d\lambda}{\int_{782}^{788} S\, d\lambda} \tag{1}$$

#151319 - $15.00 USD Received 18 Jul 2011; revised 18 Sep 2011; accepted 18 Sep 2011; published 7 Oct 2011

where S indicates the detected spectrum and λ is the wavelength. The denominator represents light that has been interacting with the tumor volume, while the nominator represents all detected light irrespectively of the tissue volume probed. A high Γ thus indicates a high spectroscopic contrast.

2.7. Intraocular pressure measurements

In order to determine the effects on intraocular pressure (IOP) caused by the force exerted on the eyeball by the fiber probe, a pressure sensor (Codman MicroSensor; Johnson & Johnson Professional, Inc., Raynham, MA) was placed within the vitreous cavity of fresh porcine eyes without tumor phantoms. This sensor is normally used to monitor the intracranial pressure after neurosurgical procedures, but has also been applied for IOP measurements [14]. The system consists of a miniature pressure transducer (diameter 1.2 mm) mounted at the tip of a flexible nylon catheter (diameter 0.7 mm), coupled to a digital pressure monitor (Codman ICP Express; Johnson & Johnson Professional, Inc., Raynham, MA) for real-time pressure readings. To facilitate placement of the pressure transducer inside the eye, a 16-gauge venflon (BD Venflon Pro; Becton Dickinson, Helsingborg, Sweden) was first passed through the optic nerve into the center of the eye. The needle was then removed, and the pressure transducer could easily be inserted through the remaining plastic tube. Thereafter, the plastic tube was withdrawn, and a 4-0 silk suture was tied around the optic nerve to prevent leakage of fluid around the catheter. The eye was placed into the gelatin bed, and the IOP changes, induced by a probe with 5 mm fiber source-detector distance and 0.5 mm fiber protrusion, were recorded in a total of 5 eyes. Prior to the fiber probe placement, the baseline IOP was set at a physiological level, between 10 and 20 mm Hg, by injecting an appropriate volume of saline into the vitreous. Three consecutive measurements at different baseline pressures were performed on each eye. As the eye was stabilized in gelatin during the measurements, the tendency of unphysiological deformation of the eye globe by the probe was reduced to a minimum.

2.8. Temperature measurements

An electronic thermometer (Bat-12; Physitemp Instruments Inc., Clifton, NJ), with an accuracy of 0.1 °C, was used to measure the temperature within the eye wall during spectroscopy. A flexible implantable thermocouple probe (IT-14; Physitemp Instruments Inc., Clifton, NJ) was inserted into the suprachoroidal space, between the inner surface of the sclera and the tumor phantom, and positioned straight below the tip of the light injecting fiber. The measurements were performed at room temperature for a duration of 15 minutes.

2.9. Scanning electron microscopy

The surfaces of the sclera of three eyes were analyzed by scanning electron microscopy (SEM) to investigate possible damage caused by the fiber probe. The eyes had been measured by a probe with 5 mm fiber source-detector distance and 0.5, 1.0 and 1.5 mm fiber protrusion, respectively. Immediately after the spectroscopic recordings, a small rectangular block of full-thickness sclera was carefully excised from the measurement area, fixed in a solution of 2% glutaraldehyde, and further processed for conventional SEM studies. Each specimen was mounted on an aluminum pin stub using conductive self-adhesive carbon labels and sputter coated with a 10 nm coating of gold-palladium. Using a scanning electron microscope (JSM-7400F; JEOL, Tokyo, Japan) the scleral surface was examined at magnifications ranging from x40 to x1250 at an accelerating voltage of 5 kV.

#151319 - $15.00 USD Received 18 Jul 2011; revised 18 Sep 2011; accepted 18 Sep 2011; published 7 Oct 2011

3. Results

3.1. Tumor phantoms

In all 6 eyes, B-scan ultrasonography revealed that the phantom was located within the suprachoroidal space, mimicking a solitary choroidal tumor with low to medium internal reflectivity. The largest basal phantom diameter (mean $\pm$ SD) was 16.0 ± 1.2 mm (range, 13.8-16.9 mm), and the largest phantom thickness (mean $\pm$ SD) was 4.7 ± 0.6 mm (range, 4.1-5.9 mm). By gross examination, the phantoms appeared as dome-shaped choroidal tumors with a light red color (Fig. 1). In previous studies, we have shown by light microscopy that the adhesive gelatin suspension lies in direct contact with the surrounding tissues [4, 5].

3.2. Noise level and dynamic range

The detector used in the optical setup had a 16 bit analog to digital resolution. With a dark current level generating around 2500 counts, it gave the detector an operational range of about 63000 levels. The dark noise level was estimated to 5.8 root mean square counts at a 10 seconds acquisition. Thus the system had a dynamic range of 11000:1, which thereby also set the limit for the maximum attenuation possible to measure in a single acquisition.

3.3. Fluorescence measure ratio

Fluorescence spectra of the porcine eyes 1-3 with varying fiber source-detector distance can be seen in Fig. 5. Note that the spectra also include the excitation light around 785 nm. Each spectrum was normalized with respect to the intensity at 785 nm. An increased contrast, meaning a higher normalized fluorescence signal, could be observed with a fiber source-detector distance of 4 and 5 mm compared to 3 mm. With a fiber source-detector distance of 6 mm, the signal was close to the noise level for the system. Maximum contrast could be measured with a fiber source-detector distance of 5 mm. Varying the fiber protrusion and measuring on eyes 4-6 resulted in the fluorescence spectra presented in Fig. 6. The trend was a declining contrast with increasing fiber protrusion, giving the maximum contrast at zero fiber protrusion.

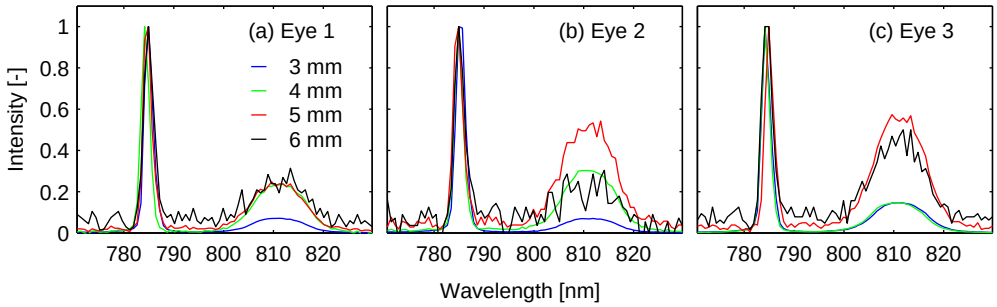

Fig. 5. Normalized fluorescence spectra for 3 porcine eyes with varying fiber source-detector distance and a fiber protrusion of 1.0 mm.

All the fluorescence measurements are summarized in Table 1, presenting the optimized contrast function, Γ. Two out of three eyes showed a maximum contrast for a fiber source-detector distance of 5 mm. One eye had peak contrast at 4 mm with still a relatively good contrast at 5 mm. Contrast as a function of fiber protrusion was maximized at zero fiber protrusion for all eyes examined and declined monotonically.

#151319 - $15.00 USD Received 18 Jul 2011; revised 18 Sep 2011; accepted 18 Sep 2011; published 7 Oct 2011

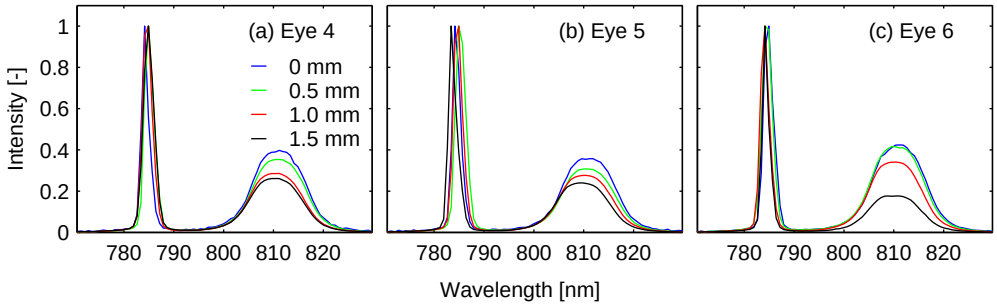

Fig. 6. Normalized fluorescence spectra for 3 porcine eyes with varying fiber protrusion and a fiber source-detector distance of 5 mm.

Table 1. Measure of the fluorescence from the stained phantom in comparison to the transmitted excitation light, Γ, in 6 different porcine eyes with varying fiber source-detector distance and fiber protrusion. The 'x' indicates the source-detector distance or protrusion used in combination with the varied source-detector distance or protrusion.

		source-detector distance [mm]				protrusion [mm]			
		3	4	5	6	0	0.5	1	1.5
eye	1	0.3	1.0	0.9	0.9			x	
	2	0.3	1.2	1.8	1.0			x	
	3	0.6	0.6	2.2	1.4			x	
	4			x		1.9	1.3	1.0	0.9
	5			x		1.5	1.1	1.1	1.1
	6			x		1.5	1.4	1.4	0.9

The photo-bleaching of the fluorophore was measured and found negible. No significant decrease of the fluorescence intensity could be observed for several seconds of exposure.

3.4. Diffuse reflectance spectroscopy

Complementary to the fluorescence measurements, transscleral spectroscopy spectra in semi-logarithmic scale for varying fiber source-detector distances are presented in Fig. 7. A clear imprint of blood and water was observable in the spectra. Oxy-hemoglobin was giving rise to the characteristic double-peak at 541 and 577 nm. The peak at 630 nm is likely to be caused by methemoglobin absorption [15]. Water could be recognized with the peak at 980 nm [16]. As expected, an increasing source-detector distance gave rise to increased attenuation. This was most evident at longer wavelengths, where the eye tissue in terms of water content is expected to be close to homogeneous. At shorter wavelengths with the longer fiber source-detector distances of 5 and 6 mm, the signal tended to drop below the noise floor.

Transscleral spectroscopy spectra with varying fiber protrusion are displayed in Fig. 8. Here the attenuation decreased with increasing fiber protrusion. At the shorter wavelengths, around 550 nm, the signal dropped below the noise floor when the fiber protrusion was less than 0.5 mm.

3.5. Intraocular pressure

The IOP elevation, induced by a probe with 5 mm fiber source-detector distance and 0.5 mm fiber protrusion, was assessed by three consecutive measurements on a total of 5 eyes. The mean

#151319 - $15.00 USD Received 18 Jul 2011; revised 18 Sep 2011; accepted 18 Sep 2011; published 7 Oct 2011

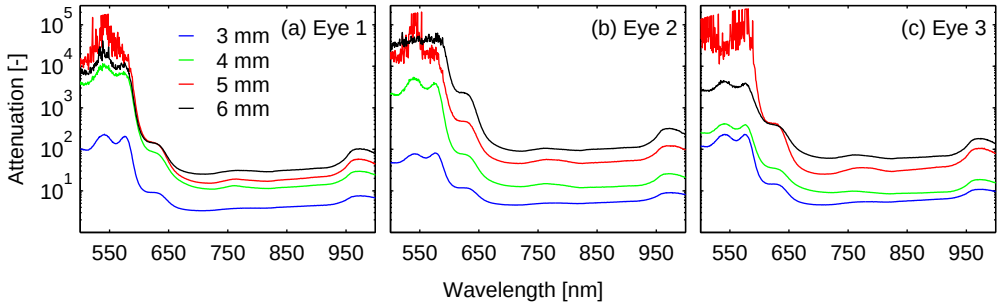

Fig. 7. Transscleral spectroscopy spectra for 3 porcine eyes with varying fiber source-detector distance and a fiber protrusion of 1.0 mm.

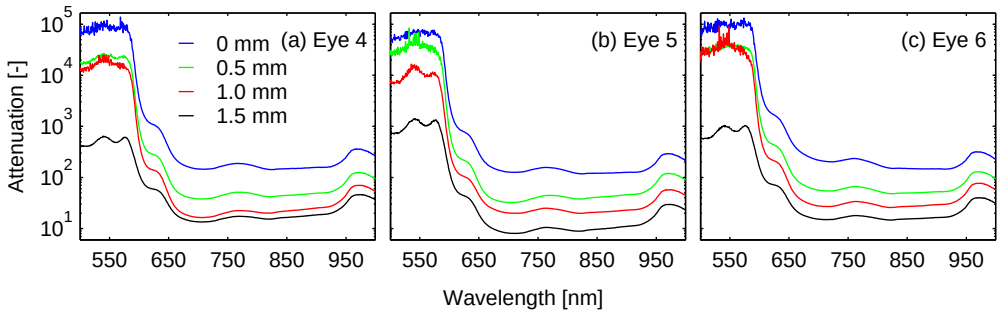

Fig. 8. Transscleral spectroscopy spectra for 3 porcine eyes with varying fiber protrusion and a fiber source-detector distance of 5 mm.

baseline pressure was 14 mm Hg (range, 10-20 mm Hg) and the mean of the maximum recorded pressure during spectroscopy was 30 mm Hg (range, 18-48 mm Hg). The force required to applanate the eye surface by the probe led to a mean pressure rise of 15 mm Hg from baseline (range, 8-28 mm Hg).

3.6. Temperature

When the light-injecting fiber was placed on the outer scleral surface and the temperature sensor was placed between the inner scleral surface and the tumor phantom, a temperature rise of only 0.3°C could be observed. The thickness of scleral tissue between the tip of the light-injecting fiber and the thermocouple was estimated to be approximately 0.5 mm.

3.7. Scanning electron microscopy

Three eyes that had been measured by a probe with 5 mm fiber source-detector distance and a fiber protrusion of 0.5, 1.0 and 1.5 mm, respectively, were examined. SEM of the excised scleral specimens revealed that there was no visible damage or persisting imprint on the scleral surface caused by the indentation of optical fibers with a protrusion of 0.5 or 1.0 mm. The case for 0.5 mm fiber protrusion and 5 mm fiber source-detector distance is shown in Fig. 9 as an example. For the eye measured with a fiber protrusion of 1.5 mm, only subtle and superficial marks could be observed on the surface of the sclera.

#151319 - $15.00 USD Received 18 Jul 2011; revised 18 Sep 2011; accepted 18 Sep 2011; published 7 Oct 2011

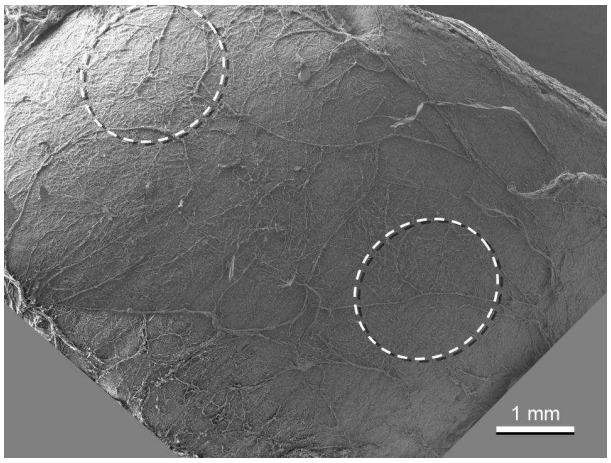

Fig. 9. Scanning electron microscopy image of the outer scleral surface from an eye that has been measured by a probe with 5 mm fiber source-detector distance and a fiber protrusion of 0.5 mm. The dashed circles indicate the areas where the optical fibers have indented the sclera. Note the plain surface and lack of any imprint from the fibers.

4. Discussion and conclusions

The central issues of this study were how to optimally design a fiber optic probe in terms of measurement geometry, usability and safety. A flexible probe was designed for this purpose in a cylindrical shape with two slightly protruding fibers. Two fiber probe parameters, the fiber source-detector distance and the fiber protrusion, were investigated as to which combination that would yield the maximum spectroscopic contrast. A fiber source-detector distance of 5 mm was found to provide maximum contrast of light interacting with the phantom relative to light propagating between the fibers without entering into the phantom volume. By the same argument, a fiber protrusion of 0 mm provided maximum spectroscopic contrast. A 5 mm source-detector distance seems reasonable considering the geometry of the eye and the highly scattering tissues. This finding is also supported by the previously published Monte-Carlo simulations [4].

The declining contrast with increasing fiber protrusion was a somewhat unexpected finding. It is, however, possible that the indentations of the two optical fibers have altered the scleral contour in a way that facilitates light transmission through the scleral layer and thus decreased the contrast. This may also be the reason for the increased attenuation of the light with decreasing protrusion. A possible explanation for the increased attenuation lays in the probe contact with the scleral surface. The probe contact, excluding the two protruding fibers, with the scleral surface would decrease as the protrusion increased. A gap would occur between the fibers and the flat surface of the probe. This gap grew bigger the more the fibers were protruding. As an effect, the scleral layer of the eye tissue did not get equally squeezed by the probe while varying the fiber protrusion. A zero fiber protrusion thereby pressed the scleral tissue layer the most and hence reduced the possible propagation pathway of the photons through the scleral tissue layer the most. At a 5 mm source-detector distance, the attenuation of a pure phantom suspensions is very strong, thereby requiring the presence of the scleral tissue layer to guide the photons. With the thickness of the scleral tissue layer being reduced with decreasing fiber protrusion, the signal magnitude hence also decreases. The slight deviations between the spectra of the six eyes were presumably caused by morphological variations, such as different degrees of pigmentation and the presence of ciliary nerves and blood vessels within the eye wall.

#151319 - $15.00 USD Received 18 Jul 2011; revised 18 Sep 2011; accepted 18 Sep 2011; published 7 Oct 2011

When considering the diffuse reflectance spectroscopy measurements with the finite dynamic range of the detector, some configurations of the fiber probe geometry were not feasible. For a source-detector distance of 5 mm, the fiber protrusion needed to be at least 1.5 mm in order to be able to measure across the entire spectral range. For a fiber protrusion of 1.0 mm, the source-detector distance could not be longer than 4 mm without being affected by the dynamic range of the detector. Limiting the spectral range would solve the issue of the finite dynamic range of the detector. Measuring a spectrum in two parts, one for the shorter wavelengths and one for the longer wavelengths, would also be a solution. The drawback of limiting the spectral range is that all chromophores of interest may not be identified. A spectrum extending to 1000 nm is required to adequately reveal water absorption [16]. Blood is strongly absorbing around 550 nm, but can also be identified at longer wavelengths [15]. Melanin extinction is most pronounced at the shorter wavelength side of the spectrum [17], even though Marchesini et al. [18] used the spectral region of 717-817 nm to quantify cutaneous melanin concentration. Thereby, a fiber probe with 5 mm source-detector distance and 0 mm fiber protrusion still has a feasible geometry, despite the limited spectral range obtainable in one acquisition for the measured tumor phantoms.

When the circular flat end of the probe applanated the sclera, it led to a relatively constant pressure exerted onto the eye surface and a stable indentation of the two optical fibers into the scleral substance. From a clinical point of view this is important, as the downward force needed is mainly defined by the IOP and the area of the probe end, and thus quite self-regulating and relatively independent of how the probe is hold by the examiner. A probe with a smaller diameter than 10 mm could perhaps be preferable (for example 7 mm diameter with 5 mm source-detector distance). However, the shorter the distance from the protruding fiber tip to the edge of the cylinder, the greater is the force required to applanate the scleral surface by the end of the probe. We investigated this in preliminary experiments by using the electronic scale, and found that the force needed for scleral applanation increased significantly with increasing source-detector distance at constant fiber protrusion (data not shown). In addition, it is probably easier to keep a thick probe steady against the eye compared to a very thin probe. During the study, we also noted that a minimal fiber protrusion of 0.5 mm could be advantageous in a clinical setting. With a slight protrusion of the fibers, the probe can be more securely held in place and it has the benefit of leaving two temporarily dark spots on the scleral surface, which may serve as a visual confirmation of placement to the examiner. The dark spots are caused by displacement of water in the scleral tissue, similar to a sponge from which water can be squeezed, making the underlying, pigmented choroid visible for a short period of time. In the present study, the eyes were prepared for spectroscopy by removing excess tissue, including the conjunctiva, from the scleral surface, and areas with a smooth surface were chosen for the measurements. In a clinical situation, however, transscleral spectroscopy may be performed with or without an overlying conjunctiva and on more uneven regions of the eye surface. Then, a slight fiber protrusion will also be beneficial to secure a close contact between the fibers and the outer scleral surface.

Because the probe will be in direct contact with the eye during spectroscopy and the method may become an integral part of ophthalmic surgery, it is important to maintain sterile conditions during the procedure. In preliminary experiments, we performed transscleral spectroscopy after covering both the probe and the fibers with a sterile, adhesive and transparent polyethylene drape (Steri-Drape 1035; 3M Health Care, St. Paul, MN). Except for a slight but insignificant reduction in the intensity of the reflected light, the sterile draping did not lead to any distinct changes in the absorption spectrum (data not shown).

In the present study, we measured real time IOP during spectroscopy. This is clinically relevant because a high probe contact pressure during the examination may induce tissue damage

#151319 - $15.00 USD Received 18 Jul 2011; revised 18 Sep 2011; accepted 18 Sep 2011; published 7 Oct 2011

and alter intraocular blood flow, leading to visual field changes [19] as well as a high degree of intra- and inter-observer variability [20]. Although we found a positive relationship between certain probe parameters and increased IOP, applanation by the preferred probe (with 5 mm source-detector distance and 0.5 mm fiber protrusion) led to a mean IOP of only 30 mm Hg with no readings above 48 mm Hg. Taking the maximum exposure time of 10 seconds into account, such brief IOP elevations are unlikely to be dangerous in non-glaucomatous individuals [21].

Porcine eyes were chosen for this study, because their anatomic and physiological features strongly resemble that of human eyes [22]. The mean scleral thickness of human eyes ranges from 0.39 to 0.49 mm [23, 24], and this corresponds closely to the porcine scleral thickness of 0.3-0.4 mm at the eye equator [25]. The phantoms were designed to simulate choroidal tumors. By injecting the gelatin suspension directly into the suprachoroidal space, we made an orthotopic model suitable for the biophysical laboratory analyses. Gelatin was chosen as the phantom matrix because of its thermo-reversible gelation behavior, making it particularly suitable for injections into the fine structures of the eye wall [26]. In addition, gelatin allows the inclusion of cellular-based constituents such as blood, and becomes both firm and adhesive after gelation, with the elastic properties similar to biological tissues [27]. To achieve scattering characteristics similar to that of the choroid, TiO_2 powder was added and homogeneously dispersed within the gelatin suspension [11, 27, 28]. The dimensions of the tumor phantoms corresponded well to the size of choroidal melanomas found in clinical studies. In a Norwegian series of 108 choroidal melanomas the mean tumor diameter and thickness were 13.3 mm (range, 4.4-21.0 mm) and 7.2 mm (range, 1.5-15.0 mm), respectively [29]. The lesion size in possible differential diagnoses, such as hemorrhagic choroidal detachment, choroidal hemangioma, metastasis and vasoproliferative tumor, is also comparable in size with the phantom dimensions in the present study [2, 3].

A fundamental challenge of biomedical optics is the validation of measurement results obtained from excised tissues. In postmortem eyes, optical properties related to physiological parameters such as blood flow, oxygenation and body temperature will change significantly. Thus, extrapolation of our results to human, *in vivo*, conditions should be done with caution. Also, the probe was optimized for a uniform tumor phantom volume with one set of optical properties. A different phantom size or different optical properties (e.g. another blood volume fraction) would probably yield a different set of optimal probe parameters. The optimization was done in the spectral range 780-800 nm. Shifting the wavelength would again change the optimal probe parameters.

In conclusion, a fiber source-detector distance of 5 mm with zero fiber protrusion was considered optimal in terms of relevant optical and spectroscopic parameters, however, the same source-detector separation with a slight fiber protrusion of 0.5 mm was found to be advantageous in a clinical setting. The study further indicates that transscleral spectroscopy can be safely performed in human eyes under *in vivo* conditions, without leading to an unacceptable IOP elevation, a significant rise in tissue temperature, or any visible damage to the scleral surface.

Acknowledgments

The study was supported by grants from the Western Norway Regional Health Authority and a Linnaeus grant for the Lund Laser Centre. The authors acknowledge Mr. Bjørn C. Lampe at the Clinical Engineering Department, Haukeland University Hospital, for manufacturing the probes used in the experiments. The scanning electron microscopy was performed at the Molecular Imaging Center (Fuge, Norwegian Research Council), University of Bergen.

#151319 - $15.00 USD Received 18 Jul 2011; revised 18 Sep 2011; accepted 18 Sep 2011; published 7 Oct 2011